Documenta Ophthalmologica **107:** 115–126, 2003.

Relationship between motion VEP and perceived velocity of gratings: effects of stimulus speed and motion adaptation

Rolf Müller[1], Gunder Bochmann[1], Mark W. Greenlee[2] & Edith Göpfert[1]
[1]*Carl Ludwig Institute of Physiology, University of Leipzig, D-04103 Leipzig, Germany;* [2]*Institute for Cognitive Science, University of Oldenburg, D-26111 Oldenburg, Germany*

Accepted 22 August 2002

Key words: motion adaptation, motion VEP, perceived speed, speed channels, stationary adaptation

Abstract

The N200 amplitude of the motion-onset VEP evoked by a parafoveal grating of variable speed (0.25–13.5°/s), constant spatial frequency (2 cpd), contrast (4%), and direction (horizontally rightward) was studied before and after adaptation to a stationary or drifting grating (1 or 4°/s). Psychophysical measurements were made simultaneously of the perceived speed. In the unadapted condition the slope of the N200 amplitude versus speed function is positive, but lower for high compared to low speeds. The N200 amplitude increases slightly after stationary adaptation. An increase in perceived speed is also evident after stationary adaptation. This increase is more pronounced for low compared to high speeds. Motion adaptation reduces N200 amplitudes over the entire speed range, whereas perceived speeds change from under-estimation to over-estimation when the speed exceeds 1.8°/s after 1°/s adaptation and 4.5°/s after 4°/s adaptation. The simultaneous evaluation of motion VEP and psychophysical results supports the view that the neurons generating the N200 component are also involved in speed perception. The data suggest the existence of a limited number (three or more) speed channels.

Introduction

Cortical neurons have been shown to be sensitive to the speed of visual stimuli [1–4]. The motion VEP reflects the activation of motion-sensitive cortical neurons. It can be evoked by sudden motion-onset of a previously stationary pattern, or sudden motion-offset of a uniformly moving pattern. Only the motion-onset VEP is considered in this paper. The evoked potential studies of motion perception in humans have concentrated on the N200 component of the motion-onset VEP [5–7]. This component exhibits amplitudes that generally increase with increasing speed of a foveal [5] or parafoveal stimulus [8]. Furthermore, the slope of the function describing the relationship between the N200 amplitude of the motion VEP and stimulus speed is generally lower for high compared to low speeds. The change in slope can be interpreted in several ways:

1. The neuronal activation that underlies the motion VEP increases over the entire perceived speed range, although this positive slope decreases at high speeds (single-channel hypothesis).
2. There are several groups of motion-sensitive neurons, which are only activated within limited speed intervals (multi-channel hypothesis: two channels, [9, 10]; three channels, [11, 12]). Neuronal connections between the channels permit an antagonistic comparison of channel activities as a processing stage for speed perception. Such an antagonistic comparison is conceivable by computation of outputs, such as the weighted average [13] or the ratio of channel activities [14].
3. Each motion-sensitive neuron constitutes its own, separate ‘channel’ (channel-continuum hypothesis [15]).

It is difficult to decide only by means of the motion VEP for or against one of these hypotheses. All the motion-sensitive neurons contribute to the ‘overall activation’ irrespective of their channel label [9], i.e., the motion VEP is label-insensitive. Assuming that there is more than one channel, the contribution

Table 1. N200 amplitude of motion VEPs evoked by a square wave grating observed through convex lenses of different refractive power (distance = 147 cm; contrast = 20%; spatial frequency = 1.4 cpd; speed = 1.8°/s; 10 subjects)

Refractive power (dpt)	N200 amplitude (μV)	
	Grand mean	Standard error
0	10.0	1.2
1.5	7.7	0.7
2.5	6.5	0.5
3.5	6.0	0.7
8.0	3.3	0.9

of each channel cannot be resolved from the overall N200 amplitude. Thus, it seems reasonable to combine VEP measurement with further motion-related data acquired simultaneously by other methods, such as magnetoencephalography, positron emission tomography, functional magnet resonance tomography, or psychophysical procedures. In this paper we attempt to elucidate the relationship between motion-onset VEP data and the cortical structures generating motion percepts by concurrent psychophysical estimates of perceived speed.

The *simultaneous* measurement of electrophysiological and psychophysical data as a condition for their common consideration is necessary, since the vigilance level varies as a function of time, and since stimulus-correlated cortical activation as well as perceptual judgment of motion are dependent, despite steady fixation, on attention [16, 17].

Adaptation can modify VEPs evoked by subsequently presented gratings [18, 19]. The N200 amplitudes of motion VEPs are reduced by prior foveal [6, 20] or parafoveal adaptation to equi-directional motion [21]. In the latter study, the adaptation effect on a grating with a moderate speed of 2°/s and a spatial frequency of 2 cpd was examined. The results suggested the existence of at least two motion channels. In the present study we have measured motion VEPs and perceived speed over a large speed range (0.25–13.5°/s) before and after stationary or motion adaptation. The aim of this paper is to obtain further knowledge about the relationship between motion VEP and perceived speed, which could also give additional information concerning the channel structure of the motion-sensitive cortical system.

Subjects and methods

Subjects

Eight subjects (three males, five females) participated in the experiments with informed and written consent. Four myopes and a hyperope wore their refractive corrections during the measurements. All subjects were naive with respect to the experimental aims. The observers viewed the stimuli binocularly at a distance of 85.5 cm. During the runs they were asked to fixate a small point presented in the centre of the display.

Stimuli

Square-wave luminance gratings of vertical orientation were created by a VSG 2/2 graphics board (Cambridge Research Ltd., Rochester, England) and presented on a high resolution display (Joyce Electronics, Cambridge, England) with a green phosphor, a frame rate of 100 Hz, and an average mean luminance of 50 cd m^{-2}. Gratings with a square-wave luminance profile were used, since they lead to a better signal-to-noise ratio in the motion VEP recordings compared to sine-wave gratings.

In a pilot experiment, a square-wave grating was blurred by convex lenses of a different refractive power. The grand means of the N200 motion VEP amplitude over 10 subjects are presented in Table 1 and suggest a contribution of higher harmonics to the motion VEP. Blurring also reduces the 25% contrast of the fundamental wave, but the N200 motion VEP amplitude is independent of contrast at values above 1–2% [7, 8, 22]. Thus, in the 8 dpt condition a moderate decrease of the N200 amplitude of the fundamental wave is conceivable at most. The contrast independence of the motion VEP above contrast values of 2% explains why sine-wave gratings with a greater contrast than in our experiments would not improve the signal-to-noise ratio. The subsequent spatial frequency specifications refer to the fundamental wave.

Procedure

Each experimental trial consisted of the sequential presentation of three stimuli, the adaptation stimulus for 5 s (at the beginning of a run for 30 s), the probe stimulus, and the match stimulus. An ISI of 1 s duration occurred prior to probe and match stimulus presentation. Both probe and match stimuli were presented for a total duration of 2 s. The stimulus

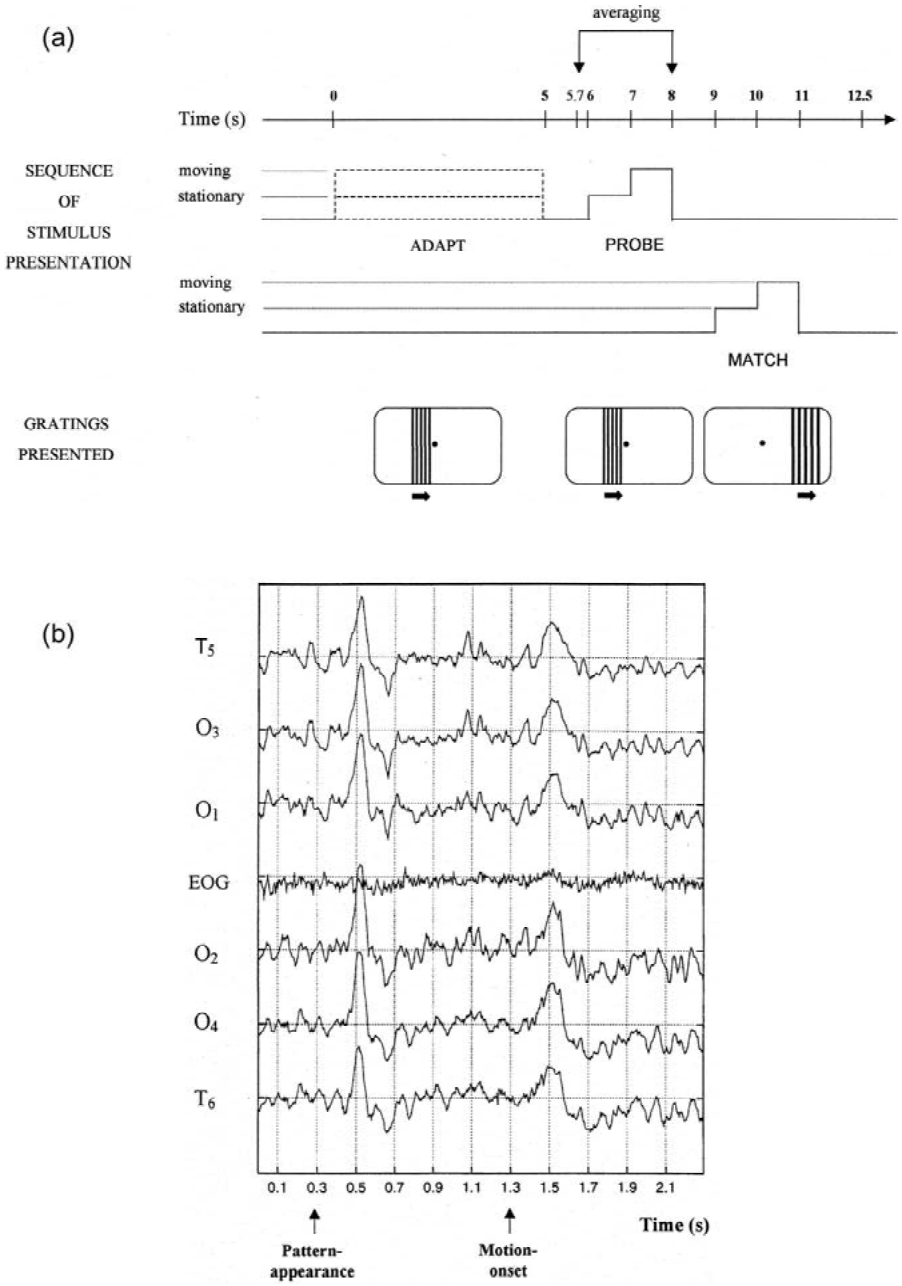

Figure 1. Panel a illustrates temporal stimulation conditions and spatial location of adaptation stimulus (ADAPT), probe stimulus (PROBE), and match stimulus (MATCH), panel b shows an example of original VEP curves. The averaged potentials ($n = 40$, subject TB) were evoked by a probe stimulus at a contrast of 4%. Pattern-appearance at 0.3 s, motion-onset at 1.3 s with a speed of 2°/s. The time interval of 2.3 s plotted in panel b corresponds to the period which is marked by 'averaging' in panel a. The vertical distance between two horizontal lines of panel b corresponds to 10 μV with negative potential differences upward. Symbols at the left designate the electrode positions from left to right on the scalp. The averaged EOG curve is given for control.

presentation consisted of a 1-s period of stationary, followed by a 1-s period of drifting presentation of the grating. An additional 1–1.5-s response period followed (see *Speed judgments*). Thus, each trial lasted 12–12.5 s (Figure 1a). Bach and Ullrich [6] and Hoffmann et al. [23] have shown that under comparable temporal conditions the N200 amplitude is reduced after adaptation.

Adaptation and probe stimuli were presented eccentrically of the fixation point. The stimulus extended from 0.5 to 3° along the horizontal meridian in one visual hemifield only. Both adaptation and probe stimuli had a height of 11° (5.5° above and below the horizontal meridian). The spatial frequency of 2 cpd lies in the medium spatial frequency range, and variations of spatial frequency within this range at constant speed should have little or no effect on the N200 motion VEP amplitude [24, 25]. The selected spatial frequency assured us that a sufficient number of periods (i.e., five) were present on the screen. At this spatial frequency, motion blurring only occurred at very high speeds.

The match stimulus subtended 4.2° in width and was presented in the opposite hemifield at an eccentricity between 3 and 7.2°. The match stimulus had the same height as the probe and adaptation stimulus, and a spatial frequency of 1.2 cpd which was adjusted to compensate for the additional eccentricity according to the cortical magnification factor. The factor was calculated with equations given by Rovamo and Virsu [26]. Note that these equations are estimated for the primary visual cortex (V1) and stationary stimuli. Results of Tootell et al. [27] suggest a similar magnification factor in human MT and V1. Thus, we felt safe to employ the same equations under our experimental conditions.

All moving stimuli drifted rightward within a stationary window (Figure 1a) and had a contrast level of 4%. The probe stimulus was presented in that hemifield where it evoked the larger motion VEP. This was the left visual hemifield in seven observers and the right visual hemifield in one observer.

Experimental conditions

Two sessions were performed in each subject for each adaptation condition. Each session consisted of four runs and in each run four probe speeds were used (0.25, 0.5, 2, 8°/s, or 0.29, 0.7, 2.8, 9.5°/s, or 0.35, 1, 4, 11.3°/s, or 0.42, 1.4, 5.7, 13.5°/s; the speed of the fastest stimulus, corresponding to a temporal frequency of 27 Hz, already approached the upper threshold of motion). These different speeds were presented in randomly interleaved staircases. Each run consisted of 80 trials with 20 presentations of each probe speed. Three conditions of adaptation were applied: unidirectional motion adaptation (speed of 1 or 4°/s), adaptation by a stationary (0°/s) pattern, or no prior adaptation. In the no-adapt condition, the time scheme remained unchanged but no adaptation stimulus was presented (blank, homogeneous screen of the same mean luminance as the gratings employed).

VEP recording

The EEG electrodes were placed left and right of O_z at locations corresponding to 5, 10, and 15% of the O_z–Fp_z head circumference away from the midline (O_1, O_3, T_5, and O_2, O_4, T_6, respectively). Linked earlobe electrodes served as reference, an electrode at the right mastoid as ground. The probe VEPs elicited by pattern-appearance and motion-onset were obtained by averaging 40 EEG responses from runs 1 and 2, and additional 40 responses from runs 3 and 4, separately. In addition, the EOG over one eye was recorded. The two EOG electrodes were situated over temporal brow and at the nose, forming a diagonal derivation with respect to the eye. Trials with eye movements, blinks, or other artifacts during probe stimulus presentation were excluded from averaging. EOG and EEG signals were amplified and averaged in the same way. We found no effect of EOG on the VEP amplitudes for the data included in the analysis.

The N200 amplitude of the motion VEP varied in size from derivation to derivation. The site with the maximal amplitude varied over subjects. In some observers, the amplitudes of T_5/T_6 exceeded the values of O_3/O_4, whereas in other observers the opposite was true. To give an overall estimation of VEP response in a hemisphere we averaged the values of the three derivations of each hemisphere. Thus, a representative N200 value of each hemisphere was obtained.

Speed judgments

During each trial, the observer judged whether the probe or the match stimulus moved faster and signalled this judgment by pressing the corresponding button on a response box. The initial speed of the match stimulus was stationary and thus perceived by all subjects as slower than the probe speed. The speed of the match stimulus was varied in dependence on the previously given response according to the 'slower-faster' variant of the Best-PEST algorithm [28], which has been shown to be appropriate for perceptual matching tasks [29]. The match stimulus speed was increased after a judgment 'probe stimulus faster' and decreased after a judgment 'match stimulus faster'. At the end of a run (after 20 decisions per probe stimulus) the perceived match stimulus speed

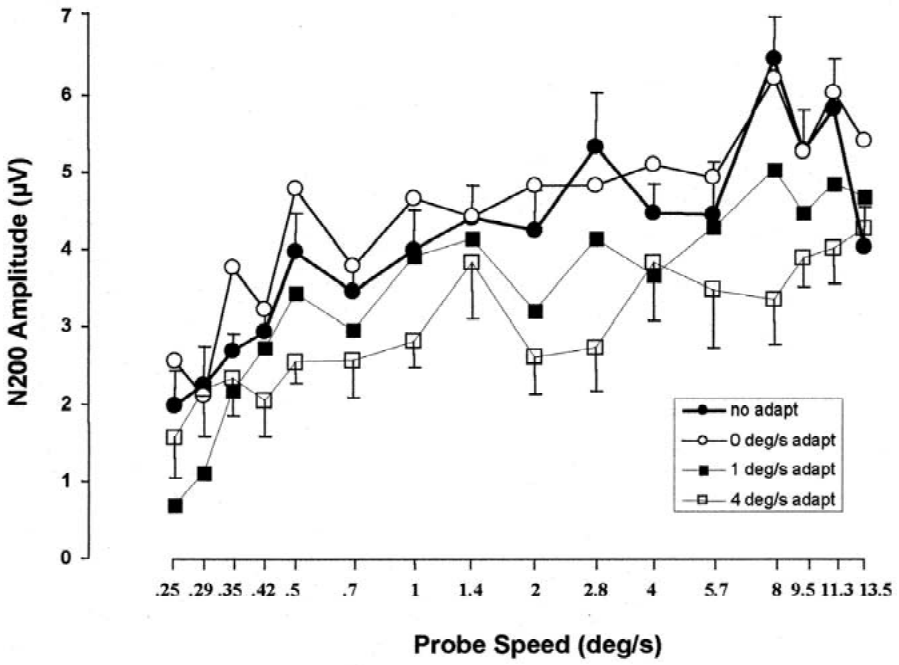

Figure 2. N200 amplitude of the motion-onset VEP as a function of probe speed (log scale) in the contralateral hemisphere. A grating with a spatial frequency of 2 cpd and a contrast of 4% moved rightward within a stationary window (eccentricity between 0.5 and 3°) in one visual hemifield. The symbols show the results without adaptation and at three adaptation conditions (see inset). The adaptation stimulus was either stationary (0°/s adapt) or it moved in the probe direction (rightward) at a speed of 1 or 4°/s. In the no-adapt condition, the time scheme remained unchanged but no adaptation stimulus was presented (blank screen). Each data point is the grand (arithmetic) mean over the averaged VEPs ($n = 40$) of eight subjects and three derivations. The vertical bars show the standard errors in the no-adapt (+1 SE) and 4°/s-adapt curve (−1 SE). The standard errors of the other curves are comparable in size and has been omitted for the sake of clarity.

corresponded to the perceived probe stimulus speed (i.e., the point of subjective equality).

Results

Figure 1b presents a registration of pattern-appearance VEPs and motion-onset VEPs without adaptation for left-hemifield stimulation from the six derivations used. The shape of pattern-appearance VEP and motion-onset VEP is similar as already reported earlier [8, 30].

Figure 2 shows the N200 amplitudes of the probe motion VEP as a function of speed (logarithmic scale) in the contralateral hemisphere. The probe stimulus was presented after the different adaptation conditions (see inset).

The results indicate the following:

1. The N200 amplitude versus probe speed (log scale) function increases with increasing speed values. The increase is evident before and after adaptation. The slope is lower for high compared to low speeds.

2. Stationary (0°/s) adaptation, compared with the no-adapt condition, elicits a significant (though, as suggested by the values of the standard errors, minimal in size) increase of the N200 amplitude (Wilcoxon test, $p < 0.01$).

3. The N200 amplitudes after 1 and 4°/s adaptation, compared with those after 0°/s adaptation, are significantly reduced (Wilcoxon test, $p < 0.01$). The effect is especially pronounced after 4°/s adaptation.

4. The corresponding ipsilateral N200 amplitudes (not plotted) are somewhat smaller than the contralateral values.

The adaptation effects in the data of Figure 2 are more clearly visible in Figures 3 and 4. The effect of stationary adaptation is plotted in Figure 3 by an N200

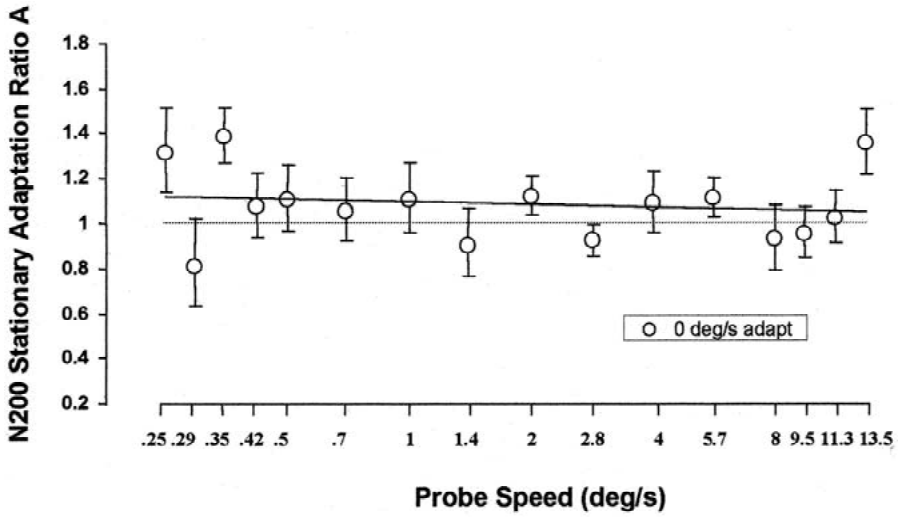

Figure 3. Stationary adaptation ratio A illustrates the relative change of the N200 amplitudes after 0°/s adaptation compared with the no-adapt values, as defined in Equation (1). The data points are calculated as geometric means with the N200 amplitude values of each subject, and these values were also used for the computation of the grand means of Figure 2. Vertical bars indicate standard errors. The continuous line was calculated by linear regression and indicates an increase of the N200 amplitudes.

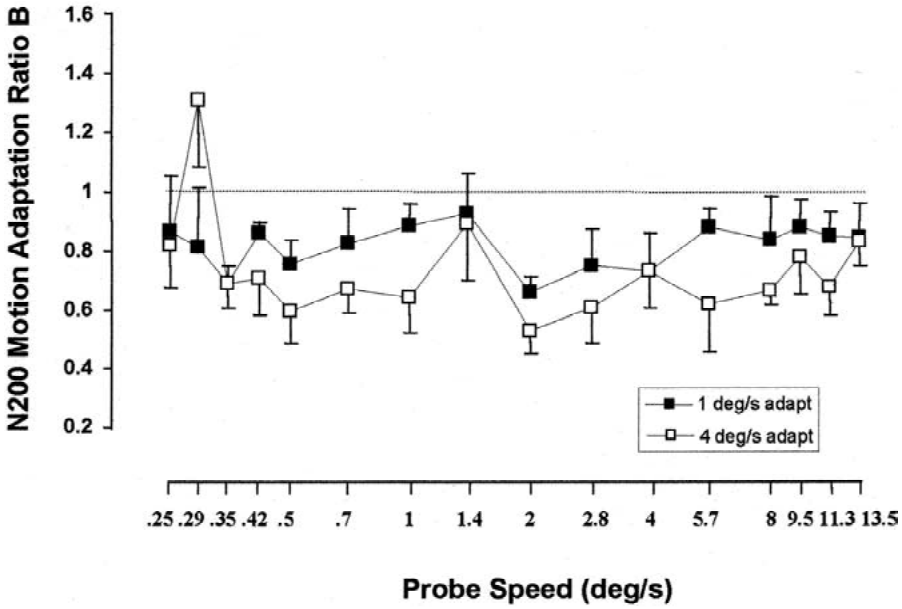

Figure 4. Motion adaptation ratio B shows the relative change of the N200 amplitudes after 1 and 4°/s adaptation compared with the 0°/s adapt values, as defined in Equation (2). The data points are calculated as geometric means with the N200 amplitude values of each subject, and these values were also used for the computation of the grand means of Figure 2. The symbols represent the adaptation conditions (see inset). Vertical bars indicate standard errors (+1 SE in the 1°/s adapt curve, −1 SE in the 4°/s adapt curve). Motion adaptation leads to an amplitude reduction.

stationary adaptation ratio

$$A = \text{N200 amplitude (0°/s adapt)} / \text{N200 amplitude (no adapt)} \quad (1)$$

as a function of speed (log scale).

The linear regression line of Figure 3 shows a slight negative slope of −0.03 and is located between $A = 1.11$ for the lowest reference speed to 1.05 for the highest speed value. A mean 8% increase of the N200 amplitude is evident due to stationary adaptation.

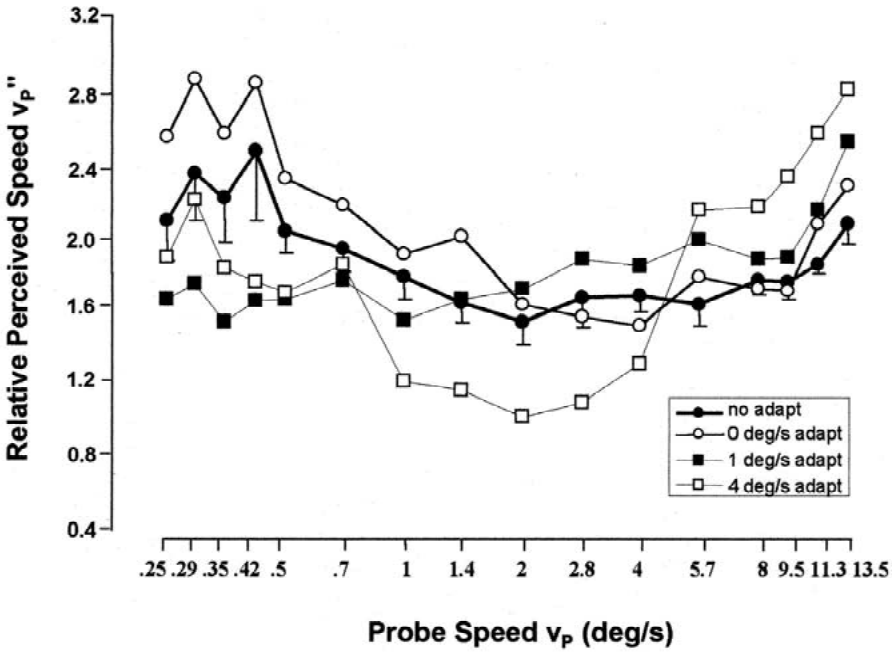

Figure 5. Relative perceived speed v_p'' of the probe stimulus, according to Equation (4), as a function of probe speed (log scale). The data points are grand (arithmetic) means over the eight observers of Figure 2. For the sake of clarity, standard error bars (−1 SE) are given only for the unadapted values, which are similar in size to the standard errors of the adapted values. The match speed v_m included in Equation (4) was estimated by the Best-PEST procedure (i.e., the perceptual match) between match and probe speed. The perceived speed matches (one value per run; two runs per subject, speed size, and adaptation state) were simultaneously acquired together with the motion VEPs of Figure 2. The symbols represent different adaptation conditions (see inset).

The effect of motion adaptation is plotted in Figure 4 by an N200 motion adaptation ratio

$$B = \text{N200 amplitude (1 or 4°/s adapt) / N200 amplitude (0°/s adapt)} \quad (2)$$

as a function of speed (log scale).

The 4°/s adaptation condition of Figure 4 exhibits significantly stronger amplitude reduction than 1°/s adaptation (Wilcoxon test, $p < 0.01$). An analysis of variance for repeated measures, with the logarithm of the N200 motion adaptation ratio B as dependent variable, indicated that the main effect of adaptation speed was significant ($F(1,202) = 4.3$; $p < 0.05$). Furthermore, the effect of probe speed on the ratio B was not significant ($F(15,202) = 1.2$; n.s.).

The psychophysical results are presented in Figure 5. The match stimulus speed v_m at the end of a run can be taken as a measure of the perceived speed v_p' of the probe stimulus (see *Speed judgment* in *Subjects and methods*):

$$v_p' \Leftrightarrow v_m. \quad (3)$$

The variable

$$v_p'' \Leftrightarrow v_m/v_p, \quad (4)$$

v_p, speed of the probe stimulus, can be considered a *relative* measure of the perceived speed of the probe stimulus. Values above unity indicate that the physical speed of the match stimulus had to be increased relative to the probe speed in order to match it perceptually, values below unity indicate that the match speed had to be decreased to match that of the probe [29].

The relative measure of the perceived speed of the probe stimulus v_p'', as defined in Equation (4), is plotted in Figure 5 as a function of probe speed (log scale). The values were acquired together with the N200 amplitudes of the motion VEPs shown in Figure 2.

As can be seen in the no-adapt curve (Figure 5, filled circles), subjects adjust relative perceived speed values of $v_p'' \approx 1.7$ at moderate probe speeds. The relative perceived speed exceeds the value of 1.7 at low probe speeds ($0.25 \leq v_p \leq 1.0$°/s) and high probe speeds ($8.0 \leq v_p \leq 13.5$°/s). The position and shape of the curve is altered after adaptation.

To describe the effect of stationary adaptation on the perceived speed we define, in analogy to Equation (1), a stationary adaptation ratio

$$A' = v_p'(0°/\text{s adapt}) \,/\, v_p' \text{ (no adapt)}. \quad (5)$$

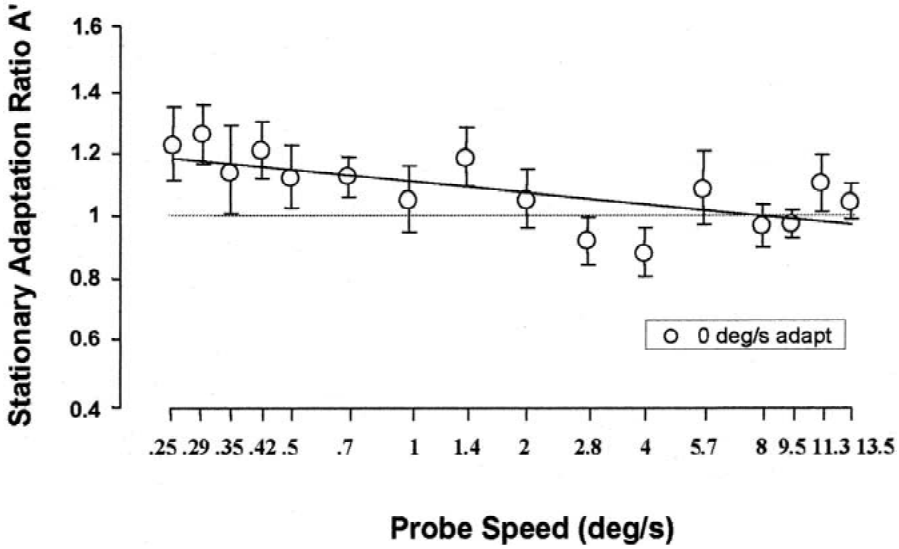

Figure 6. Stationary adaptation ratio A' shows the relative change of the perceived speed after 0°/s adaptation compared with the no-adapt values, as defined in Equation (5). The data points are calculated as geometric means with the perceived speed values of each subject, and these values were also used for the computation of the grand means of Figure 5. Vertical bars indicate standard errors. Line $A' = 1$ represents the no-adapt state. The continuous line was calculated by linear regression. Stationary adaptation gives rise to an over-estimation of the perceived speed.

The stationary adaptation ratio A' is plotted in Figure 6 as a function of probe speed (log scale).

The linear regression line of Figure 6 shows a negative slope of -0.13, and the estimation decreases from an over-estimation of 19% ($A' = 1.19$) at the lowest probe speed to an under-estimation of 3% ($A' = 0.97$) at the highest speed value. This negative slope agrees with that observed in the function describing the relationship between the N200 amplitude and the probe speed (Figure 3). Adaptation to a stationary stimulus exhibits a mean increase of 8% in the perceived speed of probe gratings in comparison with the no-adapt values. This increase in perceived speed is significant (Wilcoxon test, $p < 0.01$).

Furthermore, to describe the effect of motion adaptation on the perceived speed we define, in analogy to Equation (2), a motion adaptation ratio

$$B' = v_p' \text{ (1 or 4°/s adapt) / } v_p' \text{ (0°/s adapt).} \quad (6)$$

The motion adaptation ratio B' is shown in Figure 7 as a function of probe speed (log scale).

The 1°/s adaptation condition of Figure 7 diminishes the perceived speed of probe stimuli for speeds below 1.8°/s and enhances the perceived speed above 1.8°/s. The 4°/s adaptation condition has an effect that is comparable to that caused by 1°/s motion adaptation. The perceptual 'slowing down' effect of adaptation is more pronounced than the perceptual 'speeding up' effect. The range of transition from under-estimation to over-estimation is shifted from 1.8 to 4.5°/s after 4-°/s adaptation. An analysis of variance for repeated measures, with the logarithm of the motion adaptation ratio B' as dependent variable, indicated that the motion adaptation effect on the perceived speed (expressed by the ratio B') is strongly dependent on the speed of the probe gratings ($F(15,224) = 17.0$; $p < 0.0001$). Furthermore, the interaction between adaptation speed and probe speed was highly significant ($F(15, 224) = 3.6$; $p < 0.0001$). This interaction can be seen in Figure 7 as a shift of the functions towards higher probe speeds after adaptation to the higher adaptation speed.

Discussion

Comments on experimental design

Before we discuss the results in detail, we first comment on some important aspects of our experimental design.

Since we have kept constant the direction of motion (horizontally rightward) and spatial frequency (2 cpd) the experimental results cannot contribute to the

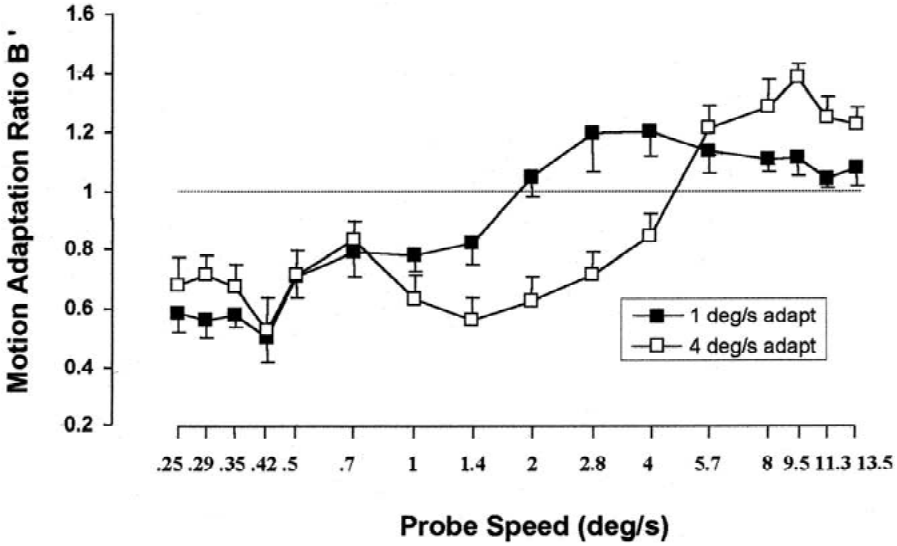

Figure 7. Motion adaptation ratio B' shows the relative change of the perceived speed after 1 and 4°/s adaptation compared with the 0°/s adapt values, as defined in Equation (6). The data points are calculated as geometric means with the perceived speed values of each subject, and these values were also used for the computation of the grand means of Figure 5. The symbols represent the adaptation conditions (see inset). Vertical bars indicate standard errors (−1 SE in the 1°/s adapt curve, +1 SE in the 4°/s adapt curve). Line $B' = 1$ represents the 0°/s adapt state. Motion adaptation leads to under-estimation at temporal frequencies below 1.8°/s (after 1°/s adapt) and 4.5°/s (after 4°/s adapt), respectively, and to over-estimation above these speed values.

question whether the channels, assuming there is more than one, respond to temporal frequency, or speed, or velocity. We will use in the following the term 'speed channel' without touching on this problem.

The averaged VEPs of Figure 1b indicate separate response components to stimulus appearance and motion onset, with a main component at peak latencies around 200 ms (N200 wave). We used as motion potential evoking stimuli an abrupt motion onset of square wave gratings. That is, on the assumption that there are channels in the spatio-temporal domain, not only neurons sensitive to the fundamental spatial and temporal frequency of the probe stimulus would contribute to motion VEP, but also neurons, sensitive to higher harmonics. In our experiments, at least the third and fifth harmonics with contrast values of 1.7 and 1%, respectively, are suitable to evoke motion VEPs [7, 8, 22]. Data of Markwardt et al. [24] and Göpfert et al. [25] indicate that N200 motion VEP amplitudes remain unchanged at constant speed in a wide spatial frequency range. Thus, activations of several spatio-temporal channels, with equal ratio of temporal to spatial frequency, contribute to the activation of a speed channel, improving the VEP signal-to-noise ratio. The pilot experiment (described in *Subjects and methods, Stimuli*) shows the size of improvement for a selected example. As a further consequence, VEP and perceived speed data can provide information about speed channels, but do not differentiate between spatio-temporal channels which constitute a speed channel [31].

The different eccentricities used for probe and match stimuli were chosen to minimize the effects of adaptation stimulus and probe stimulus, presented in one visual hemifield, on the perception of the match stimulus, presented in the opposite hemifield. Such effects could occur via commissural connections [32] or ipsilateral visual field representation due to large, mid-line spreading receptive fields of cortical neurons [33], which were also found in humans by Tootell et al. [34]. Although the comparison of gratings of unequal spatial frequency could appear, at first glance, to be more difficult, Chen et al. [35] found no measurable deterioration of speed discrimination performance under similar conditions. Our experimental design demanded a successive presentation of probe and match stimulus. Elementary stimulus parameters such as speed can be held in visual memory without loss of precision over periods up to at least 30 s [36, 37]. Thus, an impairment of speed judgment by successive stimulus presentation can be excluded under our experimental conditions.

We next discuss the experimental results in the no-adapt condition. Afterwards, we discuss the effects of adaptation on N200 amplitude and perceived speed.

No-adapt data

The no-adapt grand means of Figure 2 (filled circles) seem to support the single-channel hypothesis of motion perception. The N200 amplitude increases more or less monotonically as a function of probe speed. However, a monotonic increase of the N200 amplitude versus probe speed function is also conceivable if the motion detection system is structured into channels. If the number of neurons activated by a moving stimulus increases as a function of stimulus speed, we can expect an increase in the overall activation at transition from lower to higher speeds. This assumption holds independent of the number of channels in which the neurons are grouped. As a consequence, isolated consideration of N200 amplitudes of no-adapt motion VEPs cannot exclude any of the channel hypotheses.

The perceived probe speed $v_p{}'$ in the no-adapt condition increases as a function of probe speed v_p. The deviation from linearity is represented by $v_p{}''$ (Figure 5) which is the slope of the $v_p{}'$ curve. The u-formed shape of the $v_p{}''$ function can be taken as an argument in favour of the multi-channel hypothesis (at least three channels with optimal sensitivities in the low, moderate, and high probe speed range). Different proportions between channel activities at probe stimulus eccentricity, on the one hand, and match stimulus eccentricity, on the other hand, would explain the u-shaped function. Decreasing activities in the low-speed channel and high-speed channel as functions of eccentricity are suggested by data of Snowden and Hess [38] and Yo and Wilson [13].

Adaptation to a stationary grating

Stationary (0°/s) adaptation leads to a significant N200 amplitude increase (Figure 2; Wilcoxon test, $p < 0.01$) which is also visible in the position of the regression line above $A = 1$ (Figure 3). This result may be accounted for by inhibitory connections from the pattern-sensitive to the motion-sensitive neuronal system. The desensitization of pattern-sensitive neurons by stationary adaptation would lead to a decrease of the inhibitory effect on the motion-sensitive neurons, and, as a consequence, the overall activation of the motion-sensitive system would increase.

The increase in the N200 amplitude is accompanied by a significant increase in the perceived probe speed (Figures 5, 6; Wilcoxon test, $p < 0.01$) which seems to support the single-channel view. However, the data can also be interpreted by the multi-channel hypothesis in the following way: (1) there are inhibitory connections from pattern-sensitive to low-speed neurons; (2) the low-speed neurons constitute only one channel, and stimuli of very low speed activate only the low-speed channel, not the other channels. (That is, no antagonistic comparison would occur at very low speeds. Antagonistic comparison could not explain the increase of the perceived speed at very low probe speeds after stationary adaptation, as plotted in Figure 6. The additional effect of antagonistic comparison at moderate probe speeds leads to a reduced increase of the perceived speed after adaptation which explains the negative slope of the A' function.) Speed channels with characteristics as demanded in point 2 (one low-speed low-pass channel, one or more high-speed band-pass channels) are suggested by Mandler and Makous [12], and Hess and Snowden [39]. The effect of point 1 can be understood as an example of gain control [40, 41]. The speed overestimation of slowly moving gratings following 0°/s adaptation diminishes the motion detection threshold and improves the discrimination between stationary and moving gratings.

Motion adaptation

The effect of motion adaptation is plotted in Figure 4 by ratio B (concerning the contralateral motion VEP), and in Figure 7 by ratio B' (concerning the perceived speed). The motion adaptation effect (including conceivable interaction between pattern and motion) can be more appropriately described in relation to the 0°/s adapt data than to the no-adapt data, since the pattern-sensitive system is adapted in comparable size after 0, 2, and 8 Hz adaptation [8].

Adaptation to a grating with a speed of 1°/s reduces the N200 amplitude significantly (Wilcoxon test, $p < 0.01$) which means a reduction in the activation of motion-sensitive neurons. An even stronger adaptation effect was found after 4°/s adaptation (Figure 4). This can be explained by a further reduction of the activation of motion-sensitive neurons after 4°/s adaptation and supports the single-channel hypothesis.

However, the motion-adapt VEP data do not exclude the multi-channel hypothesis. The significantly stronger amplitude reduction following 4°/s adapta-

tion compared with 1°/s adaptation (Wilcoxon test, $p < 0.01$) can arise from smaller adaptation time constants, i.e., faster adaptation, of band-pass neurons compared with low-pass neurons. Such an assumption is used in the computation model of Smith and Edgar [14] in order to realize an optimal fit to their empirical data, and is also capable of explaining the position of the B'=1-intersection points of the curves in Figure 7 (the probe speed values exceed the adaptation speeds). The relatively small adaptation effect after 4°/s adaptation at very low probe speeds between 0.25 and 0.35°/s (Figure 4) can be taken as a further support for the multi-channel hypothesis. The 1- and 4-°/s adapt curves of Figure 4 are only slightly dependent on probe speed, which is expressed in a lack of a significant main effect in the ANOVA. The assumption of two or more speed channels would then imply a very broad channel tuning. This corresponds with findings of many authors that motion perception is based on neurons [42] and channels [43] that are more broadly tuned compared to spatial frequency channels [44].

The data discussed up to now imply the single- as well as the multi-channel hypothesis as alternative explanations for the results. The 1°/s adapt curve of Figure 7 shows an increase of the perceived speed ($B' > 1$) beyond a probe speed of 1.8°/s, the 4°/s adapt curve beyond of 4.5°/s. This result is in clear contradiction to the single-channel hypothesis, which can only explain B' values < 1. Such an increase can only be understood by taking into account the antagonistic processing of channels tuned to different speeds (e.g., Refs. [13, 14]). The 1°/s adapt curve of Figure 7 can be accounted for by the assumption of at least two broadly tuned channels. The two-channel hypothesis applied on the 4°/s adapt results of motion perception would imply weaker low-speed channel desensitization and stronger high-speed channel desensitization compared with 1°/s adaptation. This could explain the greater B' values in the low-speed range (only low-speed channel activation, no antagonistic comparison) and the lower B' values in the mid-speed range between 0.7 and 5.7°/s (antagonistic comparison). The crossing-over of the functions near the probe speed of 5.7°/s is not interpretable by two speed channels. The data can be accounted for by the assumption of a limited number, but at least of three, speed channels.

Conclusions

The simultaneously acquired data of motion VEP and perceived speed prior to and after adaptation confirm the view that the N200 motion VEP amplitude is correlated with the overall activation of all motion-sensitive cortical neurons whereas the perceived speed is, with the exception of very low speeds, determined by antagonistic comparison between the motion channels. The ambiguity of VEP data can be restricted by additional consideration of analogous psychophysical variables. Our VEP and perceived speed data taken together can be accounted for, without any contradiction, by the multi-channel hypothesis with at least three motion channels.

Acknowledgements

We thank Bengt Bartsch for his support in software development and Eva-Maria Albert for her assistance in performing the experiments and evaluating the data.

References

1. Foster KH, Gaska JP, Nagler M, Pollen DA. Spatial and temporal frequency selectivity of neurons in visual cortical areas V1 and V2 of the macaque monkey. J Physiol (London) 1985; 365: 331–63.
2. Lagae L, Raiguel S, Orban GA. Speed and direction selectivity of macaque middle temporal neurons. J Neurophysiol 1993; 69: 19–39.
3. Cheng K, Hasegawa T, Saleem KS, Tanaka K. Comparison of neuronal selectivity for stimulus speed, length, and contrast in the prestriate visual cortical areas V4 and MT of the macaque monkey. J Neurophysiol 1994; 71: 2269–80.
4. Gegenfurtner KR, Kiper DC, Levitt JB. Functional properties of neurons in macaque area V3. J Neurophysiol 1997; 77: 1906–23.
5. Göpfert E, Müller R, Markwardt F, Schlykowa L. Visuell evozierte Potentiale bei Musterbewegung. Z EEG-EMG 1983; 14: 47–51.
6. Bach M, Ullrich D. Motion adaptation governs the shape of motion-evoked cortical potentials. Vision Res 1994; 34: 1541–47.
7. Kubova Z, Kuba M, Spekreijse H, Blakemore C. Contrast dependence of motion-onset and pattern-reversal evoked potentials. Vision Res 1995; 35: 197–205.
8. Göpfert E, Müller R, Breuer D, Greenlee MW. Similarities and dissimilarities between pattern VEPs and motion VEPs. Doc Ophthalmol 1999; 97: 67–79.
9. Watson AB, Robson JG. Discrimination at threshold: labelled detectors in human vision. Vision Res 1981; 21: 1115–22.
10. Thompson P. Discrimination of moving gratings at and above detection threshold. Vision Res 1983; 23: 1533–38.
11. Mandler MB. Temporal frequency discrimination above threshold. Vision Res 1984; 24: 1873–80.

12. Mandler MB, Makous W. A three channel model of temporal frequency perception. Vision Res 1984; 24: 1881–7.
13. Yo C, Wilson HR. Peripheral temporal frequency channels code frequency and speed inaccurately but allow accurate discrimination. Vision Res 1993; 33: 33–45.
14. Smith AT, Edgar GK. Antagonistic comparison of temporal frequency filter outputs as a basis for speed perception. Vision Res 1994; 34: 253–65.
15. Schrater PR, Simoncelli EP. Local velocity representation: evidence from motion adaptation. Vision Res 1998; 38: 3899–912.
16. Torriente I, Valdes-Sosa M, Ramirez D, Bobes MA. Visual evoked potentials related to motion-onset are modulated by attention. Vision Res 1999; 39: 4122–39.
17. Smith AT, Singh KD, Greenlee MW. Attentional suppression of activity in the human visual cortex. NeuroReport 2000; 11: 271–7.
18. Mecacci L, Spinelli D. The effects of spatial frequency adaptation on human evoked potentials. Vision Res 1976; 16: 477–9.
19. Smith AT, Jeffreys DA. Size and orientation specificity of transient visual evoked potentials in man. Vision Res 1978; 18: 651–5.
20. Müller R, Göpfert E, Hartwig M. VEP-Untersuchungen zur Kodierung der Geschwindigkeit bewegter Streifenmuster im Kortex des Menschen. Z EEG-EMG 1985; 16: 75–80.
21. Müller R, Göpfert E, Breuer D, Greenlee MW. Motion VEPs with simultaneous measurement of perceived velocity. Doc Ophthalmol 1999; 97: 121–34.
22. Bach M, Ullrich D. Contrast dependency of motion-onset and pattern-reversal VEPs: Interaction of stimulus type, recording site and response component. Vision Res 1997; 37: 1845–49.
23. Hoffmann M, Dorn TJ, Bach M. Time course of motion adaptation: motion-onset visual evoked potentials and subjective estimates. Vision Res 1999; 39: 437–44.
24. Markwardt F, Göpfert E, Müller R. Influence of velocity, temporal frequency and initial phase position of grating patterns on motion VEP. Biomed Biochim Acta 1988; 47: 753–60.
25. Göpfert E, Müller R, Simon EM. The human motion onset VEP as a function of stimulation area for foveal and peripheral vision. Doc Ophthalmol 1990; 75: 165–73.
26. Rovamo J, Virsu V. An estimation and application of the human cortical magnification factor. Exp Brain Res 1979; 37: 495–510.
27. Tootell RBH, Reppas JB, Kwong KK, Malach R, Born RT, Brady TJ, Rosen BR, Belliveau JW. Functional analysis of human MT and related visual cortical areas using magnetic resonance imaging. J Neurosci 1995; 15: 3215–30.
28. Lieberman H, Pentland AP. Microcomputer-based estimation of psychophysical thresholds: the best PEST. Behav Res Methods Instrum Comput 1982; 14: 21–5.
29. Müller R, Greenlee MW. Effect of contrast and adaptation on the perception of the direction and speed of drifting gratings. Vision Res 1994; 34: 2071–92.
30. Mackie RT, McCulloch DL, Bradnam MS, Glegg M, Evans AL. The effect of motion on pattern-onset visual evoked potentials in adults and children. Doc Ophthalmol 1996; 91: 371–80.
31. Heeger DJ. Model of the extraction of image flow. J Opt Soc Am A 1987; 4: 1455–71.
32. Maunsell JHR, Van Essen DC. Topografic organization of the middle temporal visual area in the macaque monkey: representational biases and the relationship to callosal connections and myeloarchitectonic boundaries. J Comp Neurol 1987; 266: 535–55.
33. Albright TD, Desimone R. Local precision of visuotopic organization in the middle temporal area (MT) of the macaque. Exp Brain Res 1987; 65: 582–92.
34. Tootell RBH, Mendola JD, Hadjikhani NK, Liu AK, Dale AM. The representation of the ipsilateral visual field in human cerebral cortex. Proc Natl Acad Sci USA 1998; 95: 818–24.
35. Chen Y, Bedell HE, Frishman LJ. The precision of velocity discrimination across spatial frequency. Percep Psychophys 1998; 60: 1329–36.
36. Magnussen S, Greenlee MW. Retention and disruption of motion information in visual short term memory. J Exp Psychol: Learn Mem Cogn 1992; 18: 151–6.
37. Magnussen S, Greenlee MW. The psychophysics of perceptual memory. Psychol Res 1999; 62: 81–92.
38. Snowden RJ, Hess RF. Temporal frequency filters in the human peripheral visual field. Vision Res 1992; 32: 61–72.
39. Hess RF, Snowden RJ. Temporal properties of human visual filters: number, shapes and spatial covariation. Vision Res 1992; 32: 47–59.
40. Heeger DJ. Modeling simple-cell direction selectivity with normalized, half-squared, linear operators. J Neurophysiol 1993; 70: 1885–98.
41. Thomas JP, Olzak LA. Contrast gain control and fine spatial discriminations. J Opt Soc Am A 1997; 14: 2392–405.
42. Schiller PH, Logothetis K, Charles ER. Functions of the colour-opponent and broad-band channels of the visual system. Nature 1990; 343: 68–70.
43. Smith RA. Studies of temporal frequency adaptation in visual contrast sensitivity. J Physiol 1971; 216: 531–52.
44. Blakemore C, Campbell FW. On the existence of neurons in the human visual system selectively sensitive to the orientation and size of retinal images. J Physiol 1969; 203: 237–60.

Address for correspondence: R. Mueller, Carl Ludwig Institute of Physiology, University of Leipzig, Liebigstr. 27, D-04103 Leipzig, Germany
Phone: +49-341-97 15564; Fax: +49-341-97 15509; E-mail: muer@medizin.uni-leipzig.de